








Optical Rebrightening of Extragalactic Transients from the Zwicky Transient Facility

MONIKA SORAISAM ¹, THOMAS MATHESON ², CHIEN-HSIU LEE ², ABHIJIT SAHA,² GAUTHAM NARAYAN,³
NICHOLAS WOLF,² ADAM SCOTT,² STEPHANIE FIGUEROA,⁴ RAFAEL NUÑEZ,⁴ KEVIN MCKINNON ⁴,
PURAGRA GUHATHAKURTA ⁴, THOMAS G. BRINK,⁵ ALEXEI V. FILIPPENKO ^{5,6} AND NATHAN SMITH ⁷

¹NSF's National Optical-Infrared Astronomy Research Laboratory, Gemini North, 670 N Aohoku Place, Hilo, HI 96720, USA

²NSF's National Optical-Infrared Astronomy Research Laboratory, 950 N Cherry Ave, Tucson, AZ 85719, USA

³Department of Astronomy, University of Illinois at Urbana-Champaign, Urbana, IL 61801, USA

⁴Department of Astronomy & Astrophysics, University of California, Santa Cruz, 1156 High St, Santa Cruz, CA 95064, USA

⁵Department of Astronomy, University of California, 501 Campbell Hall, Berkeley, CA 94720-3411, USA

⁶Miller Institute for Basic Research in Science, University of California, Berkeley, CA 94720, USA

⁷Steward Observatory, University of Arizona, 933 N. Cherry Ave., Tucson, AZ 85721, USA

ABSTRACT

Ongoing large-scale optical time-domain surveys, such as the Zwicky Transient Facility (ZTF), are producing alerts at unprecedented rates. Analysis of transient sources has so far followed two distinct paths: archival analysis of data on transient sources at a time when they are no longer observable and real-time analysis at the time when the sources are first detected. The latter is the realm of alert brokers such as the Arizona-NOIRLab Temporal Analysis and Response to Events System (ANTARES). In this paper, we synthesize the two analysis paths and present a first systematic study of archival alert-broker data, focusing on extragalactic transients with multi-peaked light curves identified in the ANTARES archive of ZTF alerts. Our analysis yields a sample of 37 such sources, including core-collapse supernovae (with two analogs of iPTF14hls), thermonuclear supernovae interacting with their surrounding circumstellar medium, tidal disruption events, luminous blue variables, and as yet unclassified objects. A large fraction of the identified sources is currently active, warranting allocation of follow-up resources in the immediate future to further constrain their nature and the physical processes at work.

Keywords: Supernovae — variable stars — astronomy data analysis — time domain astronomy

1. INTRODUCTION

Wide-area large-scale surveys in the time domain (e.g., ASAS-SN, Shappee et al. 2014; ATLAS, Tonry et al. 2018; Zwicky Transient Facility [ZTF], Bellm et al. 2019) are increasingly pushing the frontier of astrophysical discoveries. There has been a significant transformation in the extant methodology of performing real-time science in time-domain astronomy motivated by the data deluge of the ongoing ZTF survey. To this end, software instruments, in particular alert-brokers (e.g., Saha et al. 2016; Förster et al. 2021; Matheson et al. 2021), that filter the enormous data to a manageable subset of the most interesting astrophysical events, are becoming an integral

component. For the upcoming Vera Rubin Observatory Legacy Survey of Space and Time (LSST, Ivezić et al. 2019), such specialized infrastructure will in fact be indispensable.

Early-time observations of transient events have proven to be effective in providing insights into various astrophysical processes, such as shock-breakout in Type II supernovae (SNe; Bersten et al. 2018), possible companion interaction in SNe Ia (Dimitriadis et al. 2019), etc. Equally powerful are the late-time observations of these explosive phenomena. Such observations have revealed peculiar events like nonterminal or impostor SNe that may precede actual SNe (SN 2009ip; Smith et al. 2010; Mauerhan et al. 2013) and enduring multi-peaked light curves as in the unusual SN iPTF14hls (Arcavi et al. 2017). These rare discoveries, centered on the evolution of SNe over long timescales, have been

pivotal in establishing our lack of understanding of key physical processes operating in massive-star progenitors. For example, mass loss in these stars has been plagued by uncertainties — its driving mechanisms in the early or late stages of nuclear burning are to-date not well understood (Smith 2014). However, often mass loss in these stars is the suspect for anomalous features seen in their SN explosions (Smith 2017). Precursor outbursts seen in some SNe (e.g., SN 2010mc, Ofek et al. 2013; SN 2009ip, Smith et al. 2010) have been attributed to eruptive mass-loss events in the progenitors, while interaction of SN ejecta and circumstellar material (CSM) built up by episodes of mass loss has been invoked to explain dramatic late-time bumps seen in the light curve of SN iPTF14hls (Andrews & Smith 2018).

It is clear that uncovering similar events will contribute to advancing our knowledge of these extreme phenomena and stellar evolution in general. Here, we present our results from mining the ZTF survey data with the main objective to find extragalactic transients (comprising largely SNe) with *bumpy* light curves — i.e., those with multiple peaks. In particular, we use the archival alert database of the ANTARES event broker (Matheson et al. 2021) in conjunction with the NOIR-Lab science platform Astro Data Lab¹. Many of the events we have discovered are active at the time of writing; thus, they can be monitored by the community to constrain their physical processes.

The paper is organized as follows. We describe our sample selection and modeling of the light curves in Sects. 2 and 3, respectively. Our results are shown and discussed in Sect. 4, and we conclude in Sect. 5.

2. SELECTION OF EVENTS

In order to find bumpy extragalactic events, we use the output of one of the filters running on ANTARES, viz. *HighAmp*². This is a simple filter to flag alerts from ZTF in real time displaying a significant amplitude. The amplitude is measured as the error-weighted root-mean-square (RMS) deviation about the mean of the light curve, and the threshold for flagging is set at 0.5 mag in any passband (*g* and *r* for ZTF). The output of this filter bifurcates into a transient and a variable star stream based on the absence or presence of a nearby (within 1.5'') point-like source in the template image used for subtraction. The transient stream comprises mostly extragalactic events such as SNe and active galactic nuclei (AGNs), and to a lesser extent of Galactic events

(mainly dwarf novae and classical novae). We therefore use this stream for our purpose.

There were approximately 14,500 unique sources (or loci) in the *high_amplitude_transient_candidate* output stream of ANTARES through 2021 October 15, which was the freeze date for this analysis. We consider this as our *master sample*. We post-process the loci in this sample on the Astro Data Lab science platform, which provides a JupyterLab environment and access to the archival ANTARES alert database including all the value-added products, such as annotations from cross-matching with various legacy catalogs (see Matheson et al. 2021 for details). In particular, we apply the following three selection criteria: (i) at least 10 detections in any of the ZTF passbands, (ii) all detections are positive, i.e., brightening events as compared to the template image used in subtraction, and (iii) no counterparts in the Million Quasars catalog (Flesch 2021) to filter out variability of AGNs. This resulted in 2089 loci, $\sim 14\%$ of the master sample size, which forms our penultimate sample.

We smooth the light curves of this penultimate sample and select events with multiple peaks, as described in the next section. The remaining light curves are then visually vetted to identify extragalactic explosive transients with bumpy light curves.

3. LIGHT CURVE MODELING

We use Gaussian Process (GP) regression to model the light curves of the loci from Sect. 2. GP allows for a continuous interpolation of the light curves by modeling their correlation function in a parametric way. To this end, we use *celerite* (Foreman-Mackey et al. 2017; Foreman-Mackey 2018), which provides a scalable GP implementation, ideal for the thousands of light curves in our sample.

From the available covariance functions in the *celerite* library, we opted for the series approximation of a Matern-3/2 function, parameterized by an amplitude and a timescale. We verified visually that this kernel choice returns a reasonable smoothing for most extragalactic events, although it seems to fail for some, which are mainly dwarf-nova contaminants (see Fig. 1). These edge cases can typically be identified by large uncertainty values (σ) returned by *celerite*, which also tend to be similar from time point to time point. We use this information to remove the affected loci by thresholding on the uncertainty values, dropping events for which the median σ -value is greater than 80% of the maximum σ -value.

Finally, we apply the peak-finding algorithm of *scipy*. We require the light curves in any of the two ZTF passbands to have at least one peak with a *prominence*

¹ <https://datalab.noirlab.edu/>

² The code is public and can be accessed at <https://antares.noirlab.edu/pipeline>

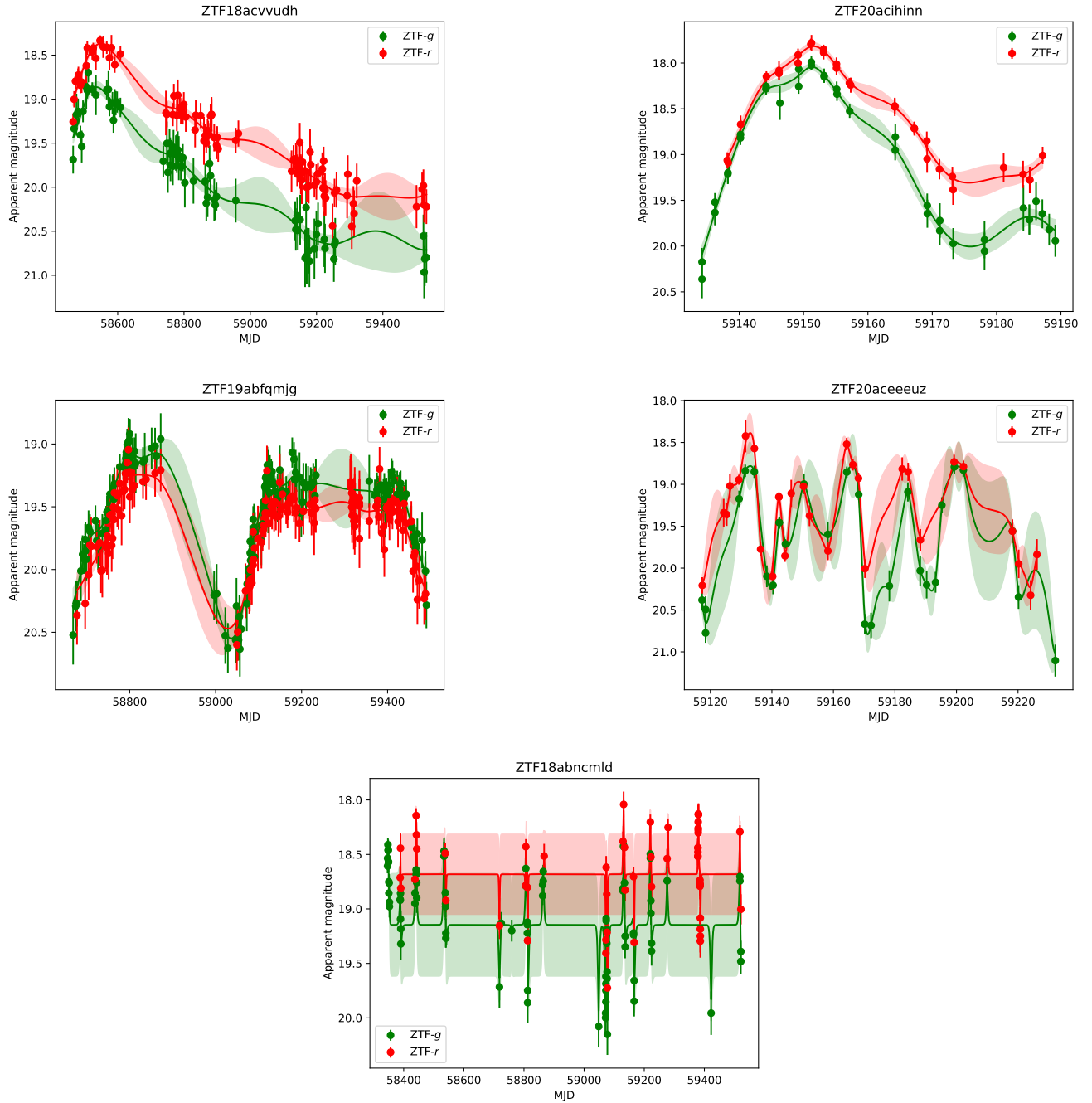


Figure 1. Example smoothed ZTF light curves. The five loci were chosen to highlight the quality of the *celerite* GP regression, which is represented by the solid lines. The green and red shaded regions show the 1σ uncertainty of the regression for the ZTF *g* and *r* passbands, respectively. The top two panels (ZTF18acvvudh, ZTF20acihinn) are SN candidates. In the middle panels, ZTF19abfqmjj is a nuclear transient candidate, while ZTF20aceeeuz has been classified as a nova in M33 (Reguitti 2020). The bottom panel is a Galactic dwarf nova (Watson et al. 2006). As is evident from the plots, the GP regression performs well for the extragalactic events, but fails for the dwarf nova.

(height between the peak and its surrounding baseline³) of greater than 0.5 mag over a timescale or width greater than 10 days. This is to ensure the presence of a prominent (i.e., SN-like) outburst in the light curve. It must *additionally* have at least one peak with a prominence greater than 0.1 mag over a width greater than 5 days. This gives us 223 loci with multiple peaks. To remove contamination from variable stars, which may be too faint in archival images used in discerning the two *HighAmp* stream (see Sect. 2), we filter out events with matches either in the Guide Star Catalog (Lasker et al. 2008), the ASAS-SN catalog of variable stars (Jayasinghe et al. 2019), or the Catalina Surveys variable star catalog (Drake et al. 2014) using ANTARES annotation. Our final sample comprises 205 events, which is just 1.4% of the master sample size. 78 of these have been typed as either SN, tidal disruption event (TDE), AGN, or luminous blue variable (LBV) on the Transient Name Server⁴.

It is to be noted that we have chosen rather permissive selection criteria above in favor of completeness, particularly for finding multiple peaks, since the photometric uncertainty can be up to 0.1 mag at the faint end, near the limit of detection of ZTF (~ 20 – 21 mag; Masci et al. 2019). We therefore further extract multiple features using the Python package feATURE eXTRACTOR FOR TIME sERIES (feets; Cabral et al. 2018) for these 205 events to investigate contaminants using the distributions of these features. We do not, however, find any significant trend that would allow us to further reduce the size of our sample. Hence, we resort to visual vetting for selecting the sources with the most clearly identifiable secondary peaks, as described in the next section.

4. RESULTS

The variation of the strength or prominence of the peak against its width for our final sample of events is shown in Fig. 2. A general trend of increasing peak strength with peak width is evident from the plot. This is likely indicative of the fact that our final sample is dominated by extragalactic transients, mainly SNe, whose light curves are known to show a similar trend.

We visually examine the light curves of the 205 sources in the final sample obtained in Sect. 3 and identify 37 with prominent bumps in their light curves, mostly corresponding to episodes of rebrightening at late times. These sources are listed in Table 1. We display the light curves of nine of these sources spanning the vari-

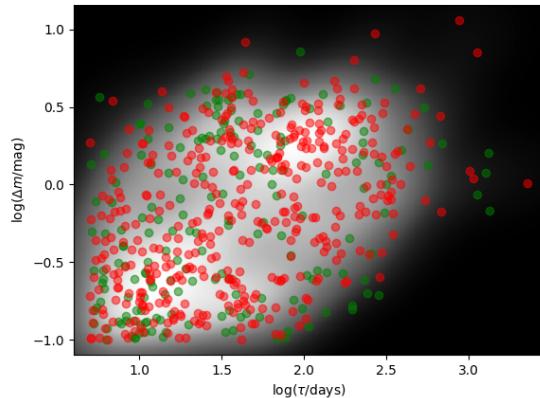


Figure 2. Variation of the prominence of the peaks, Δm , against their corresponding widths, τ , for the final sample of loci. The green and red points indicate the results for the ZTF g and r passbands, respectively, while the background shading shows the density of these points (brighter regions have higher density values).

ous categories of extragalactic transients (see below) in Fig. 3; the rest of the sources are shown in Appendix A. Some of them are currently active (e.g., SN 2019meh, SN 2020xkx, LBV 2021blu, TDE 2020acka), and can therefore be further observed to help unravel their late-time physics.

4.1. Bumpy extragalactic transient categories

- *Core-collapse supernovae:* As can be seen in Table 1, the majority of the bumpy transients are core-collapse SNe, which include stripped-envelope (SE) SNe (SNe I Ib, SNe Ib/c), SNe IIn, and superluminous SNe (SLSNe; see Filippenko 1997 and Gal-Yam 2017 for reviews of SN classification). Some of these sources exhibit light curves with double peaks at early times ($\lesssim 100$ days), such as ZTF19aamsetj/2019cad, ZTF19abxjrge/2019ply, ZTF20adadlqm/2020adnx, ZTF20aamttyw/2020cpa, ZTF21abotose/2021ugl, ZTF21aabxjqr/2021pb, ZTF21aaqvsww/2021heh, and ZTF21abghxht/2021qbc. This kind of morphology is expected for SE SNe, though it has also been seen in at least one SN IIL 2007fz (Faran et al. 2014), and the first peak is attributed to emission from the cooling envelope (see Modjaz et al. 2019, and references therein). Indeed, the examples above are mostly SE SNe, but also include a few with SN II labels (e.g., 2020cpa).

Our results also include SNe IIn and hydrogen-rich SLSNe (i.e., SLSNe-II). In particular, ZTF19abclykm/2019meh,

³ https://docs.scipy.org/doc/scipy/reference/generated/scipy.signal.peak_prominences.html

⁴ <https://www.wis-tns.org/>

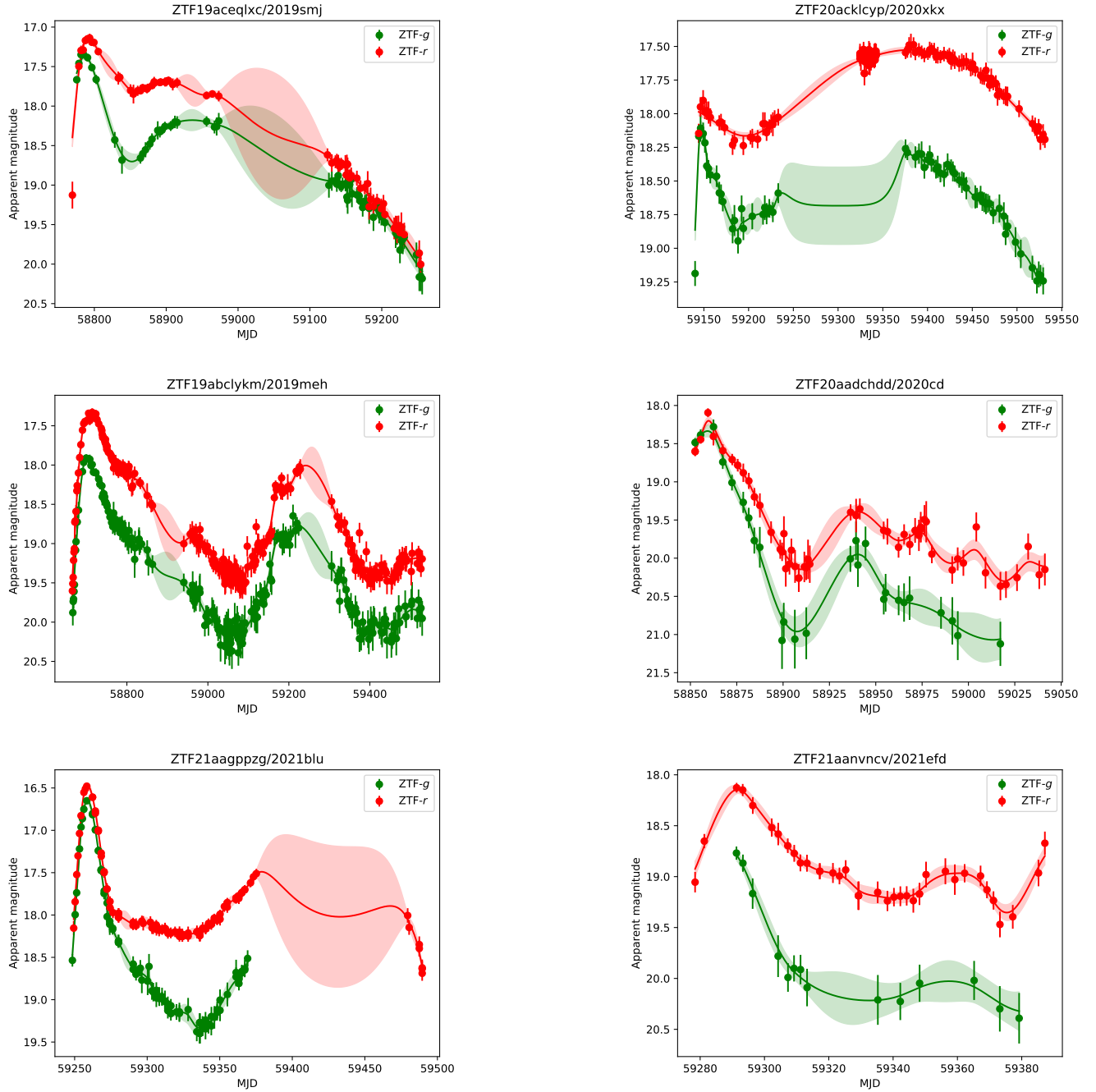


Figure 3. ZTF light curves of bumpy extragalactic transients. The lines and symbols are the same as in Fig. 1. The top two panels (ZTF19aceqlxc/2019smj, ZTF20acklcp/2020xxk) are SNe of Type II (Fremling et al. 2019; Gromadzki et al. 2020a). In the middle panels, ZTF19abclykm/2019meh is a Type II SLSN (Nicholl et al. 2019), and ZTF20aadchdd/2020cd an SN II (Dahiwalé & Fremling 2020a). In the bottom panels, ZTF21aagppzg/2021blu is an LBV in the Spider galaxy (Uno et al. 2021), and ZTF21aanvncv/2021efd an SN Ib/c (Regutti & Stritzinger 2021).

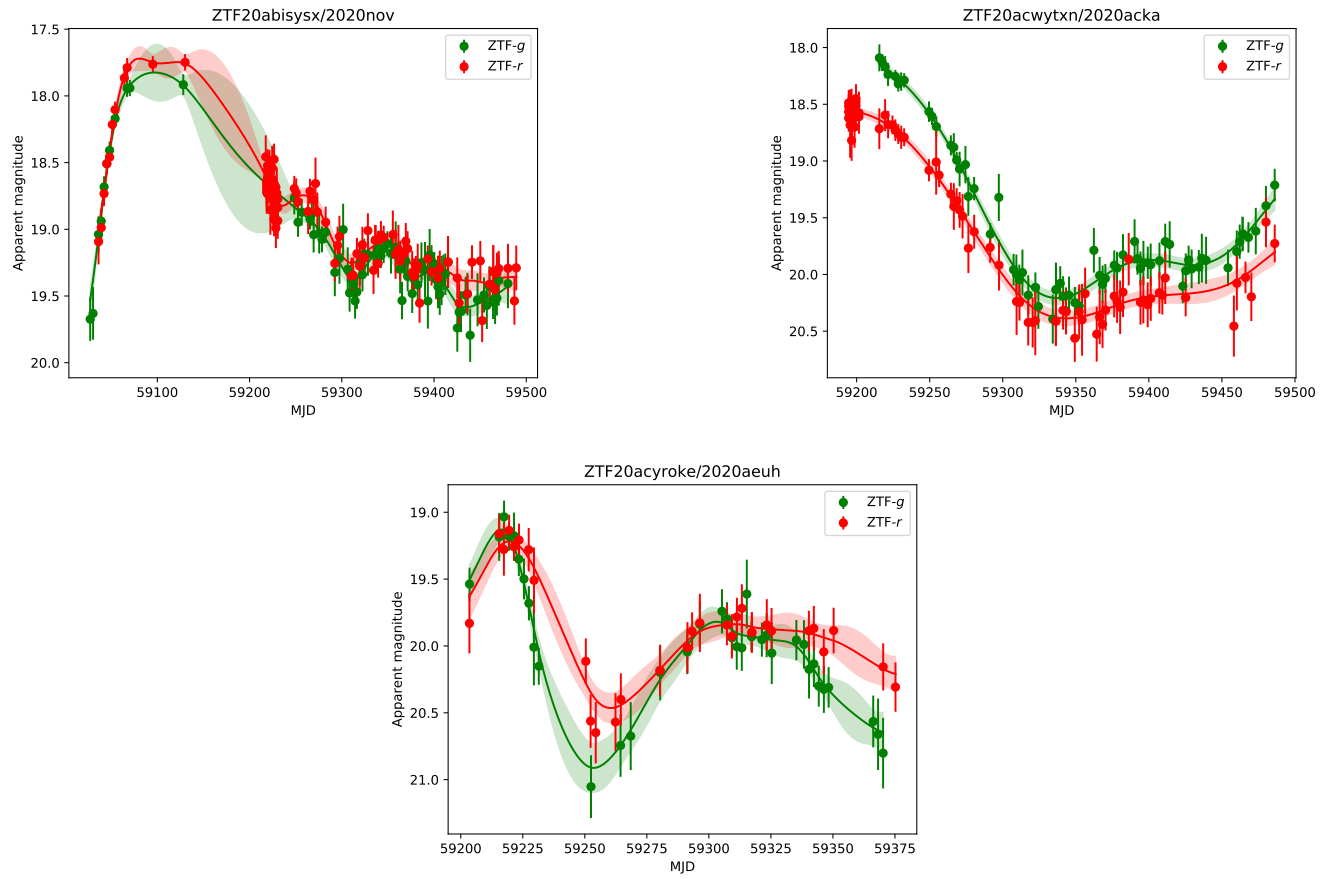


Figure 3. continued. The lines and symbols are the same as in Fig. 1. The sources in the the top panels have been typed as TDEs (ZTF20abisysx/2020nov [Dahiwale & Fremling 2020b](#); ZTF20acwytxn/2020acka [Hammerstein et al. 2021a](#)), while the source in the bottom panel is an SN Ia (2020aeuh [Weil et al. 2021](#)).

ZTF19aceqlxc/2019smj, ZTF20aacbyec/2019zrk, and ZTF20acklcyp/2020xkx exhibit prominent bumps in their late-time light curves likely powered by CSM interaction (Smith 2017). Interestingly, 2019meh (a SLSN-II) has at least three peaks — the third one currently rising (see Fig. 3), while 2020xkx (also a current event) shows two peaks, with the second one much broader ($\gtrsim 300$ days) and brighter than the first peak in the red passband.

The peak absolute magnitude of 2020xkx determined from the second peak in the red is at least $M_r = -19.02^5$ (corrected for foreground extinction using the line-of-sight reddening from Schlafly & Finkbeiner 2011). Based on a spectrum taken a few days after discovery, it was classified as an SN IIn (Gromadzki et al. 2020b). We obtained a spectrum of this event on 2021 August 12 (UT dates are used throughout this paper), 298 days after the first detection by ZTF, shown in Fig. 4. Emission lines of various species typical in such SNe are visible, prominent among which are Balmer and Paschen lines as well as the Ca II near-IR triplet. A hint of [Ca II] $\lambda\lambda 7291, 7324$ is also present. The Balmer lines exhibit broad profiles (see Fig. 4) and $H\alpha$ and $H\beta$ in particular appear to develop double peaks, pointing to the SN ejecta interacting with CSM having a disk-like geometry (Leonard et al. 2000). Its light curve, particularly the luminous peak combined with the broad shape, bears a striking resemblance to that of the peculiar iPTF14hls (Arcavi et al. 2017) and SN 2020faa (Yang et al. 2021). Continued follow-up observations of this event will be able to provide further constraints.

Another extraordinary event in our sample is SLSN-II 2019meh with a peak absolute magnitude $M_r = -22.55$. Its multiple peaks are reminiscent of iPTF14hls; however, the light curve of 2019meh appears choppier. We obtained two epochs of late-time spectra 803 and 859 days after its initial detection by ZTF, shown in Fig. 4. There is no dramatic evolution in the spectra between these two epochs. Strong emission lines of Balmer as well as Fe II are visible. We also see the presence of [S II] $\lambda\lambda 6716, 6731$, prominent in H II regions (e.g., Peimbert et al. 2017), indicating that the SN explosion likely occurred in an H II region, which

is consistent with a massive-star progenitor given the type of this SN. The shape of the $H\alpha$ profile (shown in the inset) closely resembles that of iPTF14hls seen in its late-time (+1153 d) spectrum studied by Andrews & Smith (2018). These authors attributed the unique line profile to interaction with an asymmetric (disk-like) CSM and the multiple rebrightenings in its light curve (also seen for 2019meh) to multiple shells or variation in density of the CSM. These arguments likely apply to 2019meh as well, but a comprehensive analysis of earlier and late-time follow-up observations spanning multiple wavelengths will be required for conclusive evidence.

Detailed analyses of the spectra shown here are beyond the scope of this paper. The data can be accessed at the virtual storage space of Astro Data Lab soraisam://public/spectra_bumpySNe⁶.

Our sample also contains one hydrogen-poor SLSN, ZTF20abobpcb/2020qlb (see Fig. 5). Recently, Hosseinzadeh et al. (2021) established that bumps are rather prevalent in the post-peak light curves of 34 SLSNe-I they analyzed, finding both intrinsic (i.e., the central engine) and extrinsic (CSM interaction) factors as viable explanations. 2020qlb most likely belongs to this category of SLSNe-I.

Many of the SE-SNe and SNe II in our sample also exhibit late-time (> 50 – 100 days) rebrightening in their light curves (e.g., ZTF21abcjpm/2021njo, ZTF20aadchdd/2020cd, ZTF21aanvncv/2021efd, ZTF20abxpoxd/2020sgf, ZTF19abgfuhh/2019lge), which can be ascribed to CSM interaction (see Sollerman et al. 2020, 2021; one of the SE-SNe, 2019tsf, studied by these authors has also been selected by our algorithm).

- *Thermonuclear supernovae*: The subtype of thermonuclear SNe known as SN Ia-CSM (also known as SNe Ia/IIn or SN 2002ic-like) is characterized by signatures of interaction between the SN ejecta and CSM, which include overluminous, slowly decaying light curves, with bumps in some cases (e.g., the prototype SN 2002ic; Wood-Vasey et al. 2004), and relatively narrow Balmer emission lines. We find a few bumpy transients that have been classified as SNe Ia (and SN Ia-CSM for ZTF21aaabwzx/2020aekp) in our final sam-

⁵ We do not account for host-galaxy extinction, since it is beyond the scope of this paper.

⁶ Astro Data Lab's `storeClient` library (<https://datalab.noirlab.edu/docs/api/dl.html#module-dl.storeClient>) has to be used

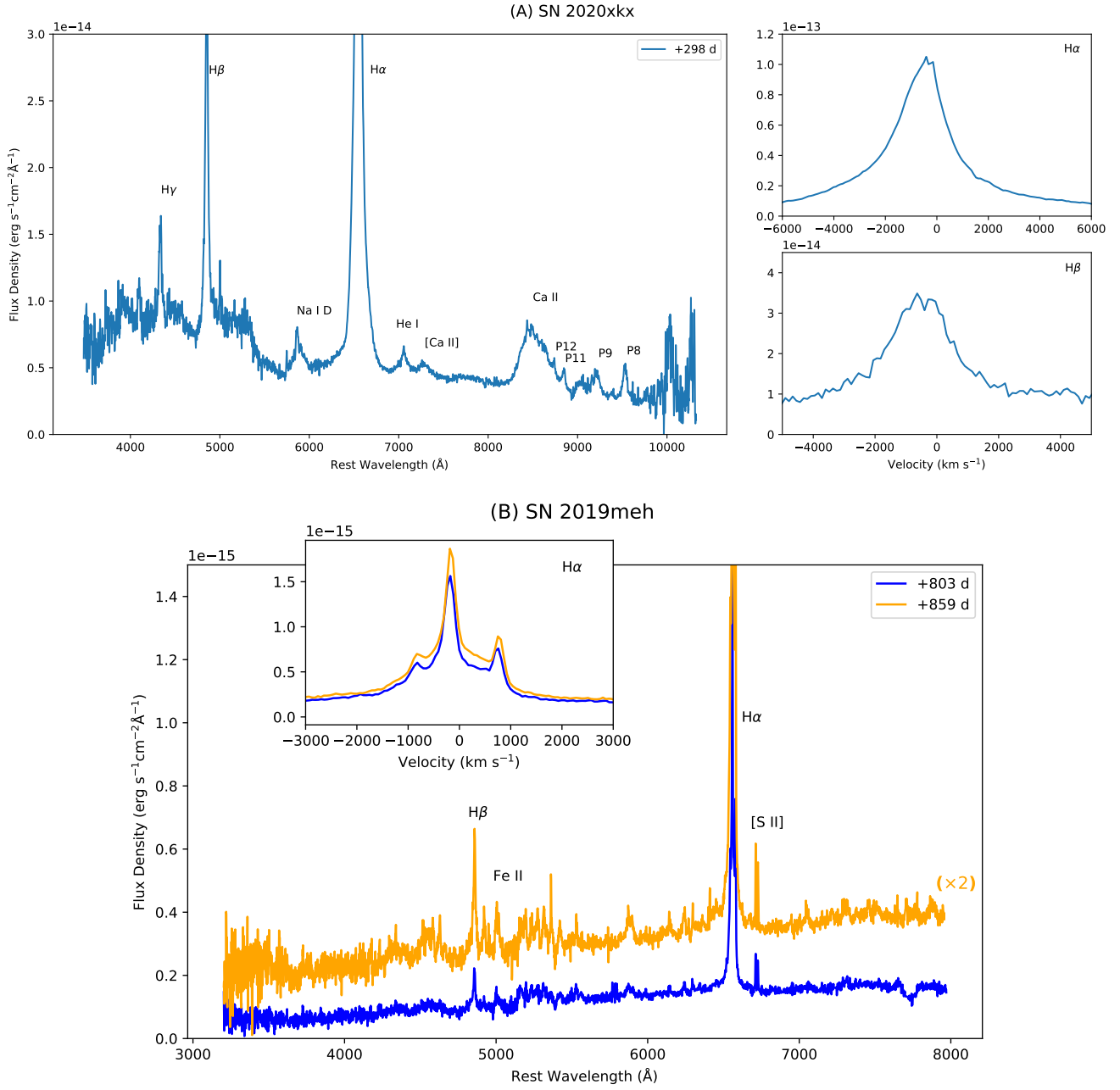


Figure 4. Late-time spectra of bumpy extragalactic transients obtained using the Kast double-beam spectrograph on the Shane 3m telescope at Lick Observatory. The epoch of the individual spectrum with respect to its first detection by ZTF is shown in the legend. The dip toward the red end (around 7800 \AA) at epoch +803 d for SN 2019meh is due to imperfect cosmic-ray removal.

ple. CSM interaction is thus the likely driver for the bumps seen in their light curves (e.g., ZTF20acyroke/2020aeuh, 2020aekp, etc.). We also obtained a spectrum of 2020aekp +253 days after first detection by ZTF (Fig. 4). A clear sign of reduced flux on the red side of H α is visible, which is typical of SNe Ia-CSM (Silverman et al. 2013).

- *Tidal disruption events (TDEs):* A few TDEs are also included in our sample — ZTF20acwytxn/2020acka, ZTF20abisysx/2020nov, and ZTF21aanxhvjv/2021-ehb. Bumps are prominent in the declining phase of the light curves for the latter two TDEs, while 2020acka exhibits a long monotonic rebrightening. TDEs are typically characterized by smoothly

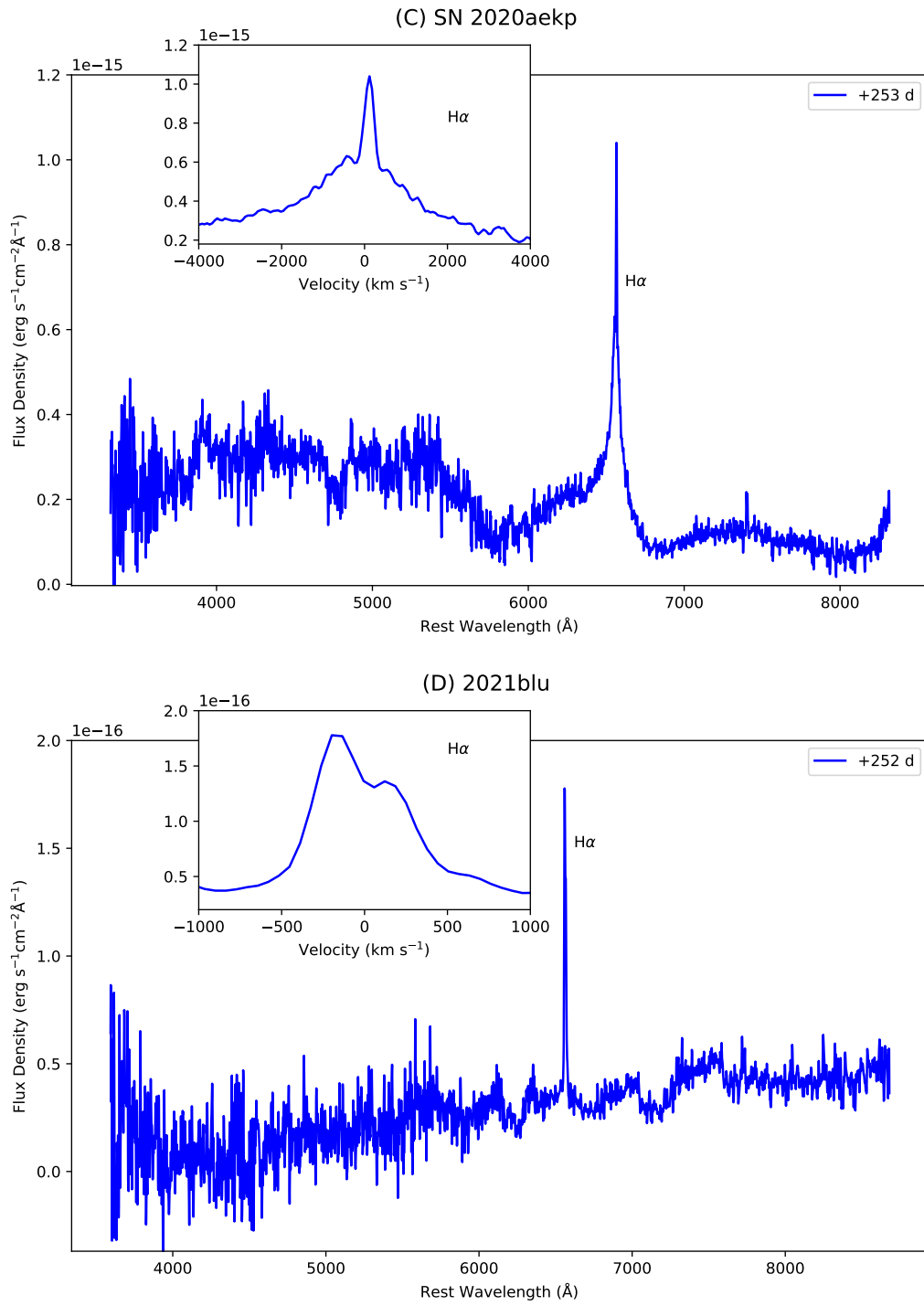


Figure 4. continued.

declining optical light curves, and the handful of discrepant examples such as PS18kh (Holoien et al. 2019) and 2018fyk/ASASSN-18ul (Wevers et al. 2019) tend to display atypical features like rebrightenings and plateaus only in their ultraviolet (UV) light curves, thought to be connected with processes in the accretion disk. The fluctuations in optical light curves shown by 2020nov and 2021ehb in our sample are perhaps similar to those seen in ASASSN-18jd, whose nature as either a TDE or a new class of nuclear transient is still unclear (Neustadt et al. 2020). The rebrightening episode of 2020acka, though classified as a TDE by Hammerstein et al. (2021b), resembles that of ZTF19abvgxrq/2019pev (also included in our sample; see below), which has been proposed as a member of the Trakhtenbrot AGN flares (Trakhtenbrot et al. 2019) by Frederick et al. (2021). These three events in our sample are currently active, and their continued late-time observations will help constrain their underlying physics.

- *Other:* Of the remaining transients in Table 1, ZTF21aagppzg/2021blu (see Fig. 3) is an LBV at redshift $z = 0.002$ in the Spider galaxy (UGC 5829). We obtained a spectrum of 2021blu with Lick Shane/Kast, 252 days after its first detection during the broad second bump, which is shown in Fig. 4. The spectrum is rather noisy; the object was quite faint (~ 19.5 mag) and the weather was poor. However, a narrow emission line from $H\alpha$ (FWHM ≈ 650 km s $^{-1}$) can be clearly seen and hints of broad metal absorption lines. 2021blu is also an ongoing event and more late-time observations will be critical to establish the nature of the second outburst — and whether it may be a terminal SN after all.

The unlabelled sources in Table 1 include ANTARES-tagged nuclear transients ZTF19abvgxrq/2019pev, ZTF19aaiqmg/2019avd, and ZTF19aaciohh/2019baf. The first two have been studied by Frederick et al. (2021) with additional follow-up data including spectroscopy and UV/X-ray observations. Based on spectroscopic similarity to AT 2017bgt, these authors have suggested 2019pev and 2019avd as members of the enhanced accretion-driven AGN flare class of Trakhtenbrot et al. (2019). 2019baf also likely belongs to this class given the similarity in its light curve evolution, even though spectroscopic observations are warranted for confirmation.

5. CONCLUSION

We have presented a first systematic study of the archival alert database of ANTARES hosted on NOIR-Lab Astro Data Lab, focusing on extragalactic transient events for which more than 10,000 unique loci were found. Modeling their light curves with Gaussian Processes, we have narrowed down the sample size to just $\sim 1.4\%$ with events showing multiple peaks or rebrightenings. From a rigorous visual vetting, we identify 37 transients with multiple prominent bumps in their light curves. These events largely fall into one of four categories: core-collapse SNe, SNe Ia-CSM, TDE/AT 2017bgt-like, and LBV outbursts. Examples include luminous SNe with iPTF14hls-like multiple peaks 2019meh and 2020xkx, and LBV 2021blu with a broad (> 100 days) rebrightening episode, which may (or may not) be related to the terminal explosion of the star. Many of these events are currently ongoing, including all the notable events mentioned above, which make them ideal candidates for late-time follow-up observations to constrain their nature. For example, iPTF14hls has demonstrated the value of such observations at multiple wavelengths (Sollerman et al. 2019). Its optical light curve shows a dramatic steep decline after ~ 1000 days, ruling out certain models such as fallback accretion and magnetars. X-ray monitoring of this object has only yielded upper limits, in contrast with other high-density CSM interaction events like SN 2010jl.

Our work demonstrates the value of mining archival time-domain data with added values from processing by the ANTARES alert-broker. With the upcoming Rubin alert data, we anticipate a richer scientific yield from ANTARES even from its archival database.

Acknowledgments: The ANTARES team gratefully acknowledges financial support from the National Science Foundation (NSF) through a cooperative agreement with the Association of Universities for Research in Astronomy (AURA) for the operation of the NSF’s National Optical-Infrared Astronomy Research Laboratory, through an NSF INSPIRE grant to the University of Arizona (CISE AST-1344024, PI: R. Snodgrass), and through a grant from the Heising-Simons Foundation (2018-0909, PI: T. Matheson). A.V.F.’s group at U.C. Berkeley is grateful for funding from the TABASGO Foundation, the Miller Institute for Basic Research in Science (where he is a Miller Senior Fellow), the Christopher J. Redlich Fund, and many individual donors. Research at Lick Observatory is partially supported by a generous gift from Google. This research uses services or data provided by the Astro Data Lab at NSF’s National Optical-Infrared Astronomy Research Laboratory.

Table 1. Extragalactic transients from ZTF with bumpy light curves

ZTF ID	RA (J2000)	DEC (J2000)	IAU Name	Type ^a	ANTARES link
ZTF18acrhegn	200.871460	27.598350	2018jbd	–	https://antares.noirlab.edu/loci/ANT2019r4lgk
ZTF19aaciohh	268.000524	65.626643	2019baf	–	https://antares.noirlab.edu/loci/ANT2019fi5vy
ZTF19aaduufr	130.748509	59.567897	2019bjr	SN IIP	https://antares.noirlab.edu/loci/ANT2020mdnsy
ZTF19aaiqmgl	125.903213	4.384020	2019avd	–	https://antares.noirlab.edu/loci/ANT2020itnzy
ZTF19aatubsj	257.278529	26.855685	2019fdr	SLSN-II	https://antares.noirlab.edu/loci/ANT2020a332y
ZTF19aamsetj	137.179054	44.812814	2019cad	SN Ic	https://antares.noirlab.edu/loci/ANT2019vndjc
ZTF19aarfkch	221.131639	70.455985	2019dwf	–	https://antares.noirlab.edu/loci/ANT2019pjqws
ZTF19abclykm	321.822735	64.416439	2019meh	SLSN-II	https://antares.noirlab.edu/loci/ANT2020agsa4
ZTF19abgfuhh	3.725184	36.300906	2019lgc	SN Iib	https://antares.noirlab.edu/loci/ANT2019lpafi
ZTF19abvgxrq	67.344703	0.618760	2019pev	–	https://antares.noirlab.edu/loci/ANT2020pfqji
ZTF19abxjrge	44.945755	15.296852	2019ply	SN Iib	https://antares.noirlab.edu/loci/ANT2020unoti
ZTF19aceqlxc	117.419663	5.074203	2019smj	SN IIn	https://antares.noirlab.edu/loci/ANT2020edwny
ZTF19ackjszs	167.136636	-10.481770	2019tsf	SN Ib	https://antares.noirlab.edu/loci/ANT2020hnhs6
ZTF20aacbyec	174.947491	19.929643	2019zrk	SN IIn	https://antares.noirlab.edu/loci/ANT2020bq46c
ZTF20aadchdd	203.234621	54.042149	2020cd	SN II	https://antares.noirlab.edu/loci/ANT2020alxje
ZTF20aamttyw	261.657181	38.208176	2020cpa	SN II	https://antares.noirlab.edu/loci/ANT2020mosa
ZTF20aarvuvj	265.952909	22.426205	2020dvd	–	https://antares.noirlab.edu/loci/ANT2020amjjs
ZTF20aatxryt	167.946571	29.385115	2020eyj	SN Ia	https://antares.noirlab.edu/loci/ANT2020as3vu
ZTF20abisysx	254.554098	2.117527	2020nov	TDE	https://antares.noirlab.edu/loci/ANT2020dxbmq
ZTF20abobpcb	286.956514	62.963752	2020qlb	SLSN-I	https://antares.noirlab.edu/loci/ANT2020nzw4s
ZTF20abxpoxd	50.719846	42.556106	2020sgf	SN Ic	https://antares.noirlab.edu/loci/ANT202024yj2
ZTF20acihinn	340.694664	51.505972	2020vzz	–	https://antares.noirlab.edu/loci/ANT2020aefccmq
ZTF20acklcyp	350.117382	22.986906	2020xkx	SN IIn	https://antares.noirlab.edu/loci/ANT2020aekfzhy
ZTF20acwytxn	238.758128	16.304531	2020acka	TDE	https://antares.noirlab.edu/loci/ANT2020afjo7na
ZTF20acxqaof	84.822243	63.641719	2020uly	SN Ia	https://antares.noirlab.edu/loci/ANT20207mb5a
ZTF20acyroke	188.966056	37.703481	2020aeuh	SN Ia	https://antares.noirlab.edu/loci/ANT2020afmdwmy
ZTF20adadlqm	46.481311	41.608693	2020adnx	SN II	https://antares.noirlab.edu/loci/ANT2020afo32ha
ZTF21aaabwzx	235.797447	17.813116	2020aekp	SN Ia-CSM	https://antares.noirlab.edu/loci/ANT2021mqlq
ZTF21aabxjqr	146.194990	51.687393	2021pb	SN Iib	https://antares.noirlab.edu/loci/ANT2021bbfmu
ZTF21aagppzg	160.643112	34.437380	2021blu	LBV	https://antares.noirlab.edu/loci/ANT2021djjs2
ZTF21aaqsvvw	119.947061	25.355832	2021heh	SN Iib	https://antares.noirlab.edu/loci/ANT2021ixxiq
ZTF21aanvncv	171.102978	23.649608	2021efd	SN Ib/c	https://antares.noirlab.edu/loci/ANT2021hgwrn
ZTF21aanxhvj	46.949254	40.311343	2021ehb	TDE	https://antares.noirlab.edu/loci/ANT2021hhxq6
ZTF21abcjpnm	241.779105	47.443639	2021njo	SN II	https://antares.noirlab.edu/loci/ANT2021n6cbs
ZTF21abfjlx	218.342847	19.128498	2021pkd	SN Iib	https://antares.noirlab.edu/loci/ANT2021pt3zq
ZTF21abghxht	292.510897	35.046311	2021qbc	SN II-pec	https://antares.noirlab.edu/loci/ANT2021qc32w
ZTF21abotose	246.982038	20.253160	2021ugl	SN Iib	https://antares.noirlab.edu/loci/ANT2021uuv34

^aClassification, if available, is obtained from the Transient Name Server (<https://www.wis-tns.org/>). The redshift information for these events can be seen using the ANTARES link.

Software: `numpy` (van der Walt et al. 2011), `scipy` (Jones et al. 2001–), `astropy` (Astropy Collaboration et al. 2013), `matplotlib` (Hunter 2007)

REFERENCES

- Andrews, J. E., & Smith, N. 2018, *MNRAS*, 477, 74, doi: [10.1093/mnras/sty584](https://doi.org/10.1093/mnras/sty584)
- Arcavi, I., Howell, D. A., Kasen, D., et al. 2017, *Nature*, 551, 210, doi: [10.1038/nature24030](https://doi.org/10.1038/nature24030)
- Astropy Collaboration, Robitaille, T. P., Tollerud, E. J., et al. 2013, *A&A*, 558, A33, doi: [10.1051/0004-6361/201322068](https://doi.org/10.1051/0004-6361/201322068)
- Bellm, E. C., Kulkarni, S. R., Graham, M. J., et al. 2019, *PASP*, 131, 018002, doi: [10.1088/1538-3873/aaecbe](https://doi.org/10.1088/1538-3873/aaecbe)
- Bersten, M. C., Folatelli, G., García, F., et al. 2018, *Nature*, 554, 497, doi: [10.1038/nature25151](https://doi.org/10.1038/nature25151)
- Cabral, J. B., Sánchez, B., Ramos, F., et al. 2018, *Astronomy and Computing*, 25, 213, doi: [10.1016/j.ascom.2018.09.005](https://doi.org/10.1016/j.ascom.2018.09.005)
- Dahiwale, A., & Fremling, C. 2020a, *Transient Name Server Classification Report*, 2020-204, 1
- . 2020b, *Transient Name Server Classification Report*, 2020-3800, 1
- Dimitriadis, G., Foley, R. J., Rest, A., et al. 2019, *ApJL*, 870, L1, doi: [10.3847/2041-8213/aaedb0](https://doi.org/10.3847/2041-8213/aaedb0)
- Drake, A. J., Graham, M. J., Djorgovski, S. G., et al. 2014, *ApJS*, 213, 9, doi: [10.1088/0067-0049/213/1/9](https://doi.org/10.1088/0067-0049/213/1/9)
- Faran, T., Poznanski, D., Filippenko, A. V., et al. 2014, *MNRAS*, 445, 554, doi: [10.1093/mnras/stu1760](https://doi.org/10.1093/mnras/stu1760)
- Filippenko, A. V. 1997, *ARA&A*, 35, 309, doi: [10.1146/annurev.astro.35.1.309](https://doi.org/10.1146/annurev.astro.35.1.309)
- Flesch, E. W. 2021, arXiv e-prints, arXiv:2105.12985. <https://arxiv.org/abs/2105.12985>
- Foreman-Mackey, D. 2018, *Research Notes of the American Astronomical Society*, 2, 31, doi: [10.3847/2515-5172/aaaf6c](https://doi.org/10.3847/2515-5172/aaaf6c)
- Foreman-Mackey, D., Agol, E., Ambikasaran, S., & Angus, R. 2017, *AJ*, 154, 220, doi: [10.3847/1538-3881/aa9332](https://doi.org/10.3847/1538-3881/aa9332)
- Förster, F., Cabrera-Vives, G., Castillo-Navarrete, E., et al. 2021, *AJ*, 161, 242, doi: [10.3847/1538-3881/abe9bc](https://doi.org/10.3847/1538-3881/abe9bc)
- Frederick, S., Gezari, S., Graham, M. J., et al. 2021, *ApJ*, 920, 56, doi: [10.3847/1538-4357/ac110f](https://doi.org/10.3847/1538-4357/ac110f)
- Fremling, C., Sharma, Y., & Dahiwale, A. 2019, *Transient Name Server Classification Report*, 2019-2297, 1
- Gal-Yam, A. 2017, *Observational and Physical Classification of Supernovae*, ed. A. W. Alsabti & P. Murdin, 195, doi: [10.1007/978-3-319-21846-5_35](https://doi.org/10.1007/978-3-319-21846-5_35)
- Gromadzki, M., Ihanec, N., Callis, E., & Yaron, O. 2020a, *Transient Name Server Classification Report*, 2020-3243, 1
- . 2020b, *Transient Name Server Classification Report*, 2020-3243, 1
- Hammerstein, E., Gezari, S., Velzen, S. V., et al. 2021a, *Transient Name Server Classification Report*, 2021-262, 1
- . 2021b, *Transient Name Server Classification Report*, 2021-262, 1
- Holoien, T. W. S., Huber, M. E., Shappee, B. J., et al. 2019, *ApJ*, 880, 120, doi: [10.3847/1538-4357/ab2ae1](https://doi.org/10.3847/1538-4357/ab2ae1)
- Hosseinzadeh, G., Berger, E., Metzger, B. D., et al. 2021, arXiv e-prints, arXiv:2109.09743. <https://arxiv.org/abs/2109.09743>
- Hunter, J. D. 2007, *Computing In Science & Engineering*, 9, 90, doi: [10.1109/MCSE.2007.55](https://doi.org/10.1109/MCSE.2007.55)
- Ivezić, Ž., Kahn, S. M., Tyson, J. A., et al. 2019, *ApJ*, 873, 111, doi: [10.3847/1538-4357/ab042c](https://doi.org/10.3847/1538-4357/ab042c)
- Jayasinghe, T., Stanek, K. Z., Kochanek, C. S., et al. 2019, *MNRAS*, 486, 1907, doi: [10.1093/mnras/stz844](https://doi.org/10.1093/mnras/stz844)
- Jones, E., Oliphant, T., Peterson, P., et al. 2001–, *SciPy: Open source scientific tools for Python*. <http://www.scipy.org/>
- Lasker, B. M., Lattanzi, M. G., McLean, B. J., et al. 2008, *AJ*, 136, 735, doi: [10.1088/0004-6256/136/2/735](https://doi.org/10.1088/0004-6256/136/2/735)
- Leonard, D. C., Filippenko, A. V., Barth, A. J., & Matheson, T. 2000, *ApJ*, 536, 239, doi: [10.1086/308910](https://doi.org/10.1086/308910)
- Masci, F. J., Laher, R. R., Rusholme, B., et al. 2019, *PASP*, 131, 018003, doi: [10.1088/1538-3873/aae8ac](https://doi.org/10.1088/1538-3873/aae8ac)
- Matheson, T., Stubens, C., Wolf, N., et al. 2021, *AJ*, 161, 107, doi: [10.3847/1538-3881/abd703](https://doi.org/10.3847/1538-3881/abd703)
- Mauerhan, J. C., Smith, N., Filippenko, A. V., et al. 2013, *MNRAS*, 430, 1801, doi: [10.1093/mnras/stt009](https://doi.org/10.1093/mnras/stt009)
- Modjaz, M., Gutiérrez, C. P., & Arcavi, I. 2019, *Nature Astronomy*, 3, 717, doi: [10.1038/s41550-019-0856-2](https://doi.org/10.1038/s41550-019-0856-2)
- Neustadt, J. M. M., Holoien, T. W. S., Kochanek, C. S., et al. 2020, *MNRAS*, 494, 2538, doi: [10.1093/mnras/staa859](https://doi.org/10.1093/mnras/staa859)
- Nicholl, M., Short, P., Lawrence, A., Ross, N., & Smartt, S. 2019, *Transient Name Server Classification Report*, 2019-1586, 1
- Ofek, E. O., Sullivan, M., Cenko, S. B., et al. 2013, *Nature*, 494, 65, doi: [10.1038/nature11877](https://doi.org/10.1038/nature11877)

- Peimbert, M., Peimbert, A., & Delgado-Inglada, G. 2017, *PASP*, 129, 082001, doi: [10.1088/1538-3873/aa72c3](https://doi.org/10.1088/1538-3873/aa72c3)
- Reguitti, A. 2020, *Transient Name Server Classification Report*, 2020-3825, 1
- Reguitti, A., & Stritzinger, M. 2021, *Transient Name Server Classification Report*, 2021-682, 1
- Saha, A., Wang, Z., Matheson, T., et al. 2016, in *Society of Photo-Optical Instrumentation Engineers (SPIE) Conference Series*, Vol. 9910, *Observatory Operations: Strategies, Processes, and Systems VI*, ed. A. B. Peck, R. L. Seaman, & C. R. Benn, 99100F, doi: [10.1117/12.2232095](https://doi.org/10.1117/12.2232095)
- Schlafly, E. F., & Finkbeiner, D. P. 2011, *ApJ*, 737, 103, doi: [10.1088/0004-637X/737/2/103](https://doi.org/10.1088/0004-637X/737/2/103)
- Shappee, B. J., Prieto, J. L., Grupe, D., et al. 2014, *ApJ*, 788, 48, doi: [10.1088/0004-637X/788/1/48](https://doi.org/10.1088/0004-637X/788/1/48)
- Silverman, J. M., Nugent, P. E., Gal-Yam, A., et al. 2013, *ApJS*, 207, 3, doi: [10.1088/0067-0049/207/1/3](https://doi.org/10.1088/0067-0049/207/1/3)
- Smith, N. 2014, *ARA&A*, 52, 487, doi: [10.1146/annurev-astro-081913-040025](https://doi.org/10.1146/annurev-astro-081913-040025)
- . 2017, *Interacting Supernovae: Types II_n and Ibn*, ed. A. W. Alsabti & P. Murdin, 403, doi: [10.1007/978-3-319-21846-5_38](https://doi.org/10.1007/978-3-319-21846-5_38)
- Smith, N., Miller, A., Li, W., et al. 2010, *AJ*, 139, 1451, doi: [10.1088/0004-6256/139/4/1451](https://doi.org/10.1088/0004-6256/139/4/1451)
- Sollerman, J., Taddia, F., Arcavi, I., et al. 2019, *A&A*, 621, A30, doi: [10.1051/0004-6361/201833689](https://doi.org/10.1051/0004-6361/201833689)
- Sollerman, J., Fransson, C., Barbarino, C., et al. 2020, *A&A*, 643, A79, doi: [10.1051/0004-6361/202038960](https://doi.org/10.1051/0004-6361/202038960)
- Sollerman, J., Yang, S., Schulze, S., et al. 2021, *arXiv e-prints*, arXiv:2107.14503, <https://arxiv.org/abs/2107.14503>
- Tonry, J. L., Denneau, L., Heinze, A. N., et al. 2018, *PASP*, 130, 064505, doi: [10.1088/1538-3873/aabadf](https://doi.org/10.1088/1538-3873/aabadf)
- Trakhtenbrot, B., Arcavi, I., Ricci, C., et al. 2019, *Nature Astronomy*, 3, 242, doi: [10.1038/s41550-018-0661-3](https://doi.org/10.1038/s41550-018-0661-3)
- Uno, K., Kawabata, M., & Taguchi, K. 2021, *Transient Name Server Classification Report*, 2021-393, 1
- van der Walt, S., Colbert, S. C., & Varoquaux, G. 2011, *Computing In Science & Engineering*, 13, 22, doi: [10.1109/MCSE.2011.37](https://doi.org/10.1109/MCSE.2011.37)
- Watson, C. L., Henden, A. A., & Price, A. 2006, *Society for Astronomical Sciences Annual Symposium*, 25, 47
- Weil, K. E., Subrayan, B. M., & Milisavljevic, D. 2021, *Transient Name Server Classification Report*, 2021-812, 1
- Wevers, T., Pasham, D. R., van Velzen, S., et al. 2019, *MNRAS*, 488, 4816, doi: [10.1093/mnras/stz1976](https://doi.org/10.1093/mnras/stz1976)
- Wood-Vasey, W. M., Wang, L., & Aldering, G. 2004, *ApJ*, 616, 339, doi: [10.1086/424826](https://doi.org/10.1086/424826)
- Yang, S., Sollerman, J., Chen, T. W., et al. 2021, *A&A*, 646, A22, doi: [10.1051/0004-6361/202039440](https://doi.org/10.1051/0004-6361/202039440)

APPENDIX

A. EXTRAGALACTIC TRANSIENTS WITH BUMPY LIGHT CURVES

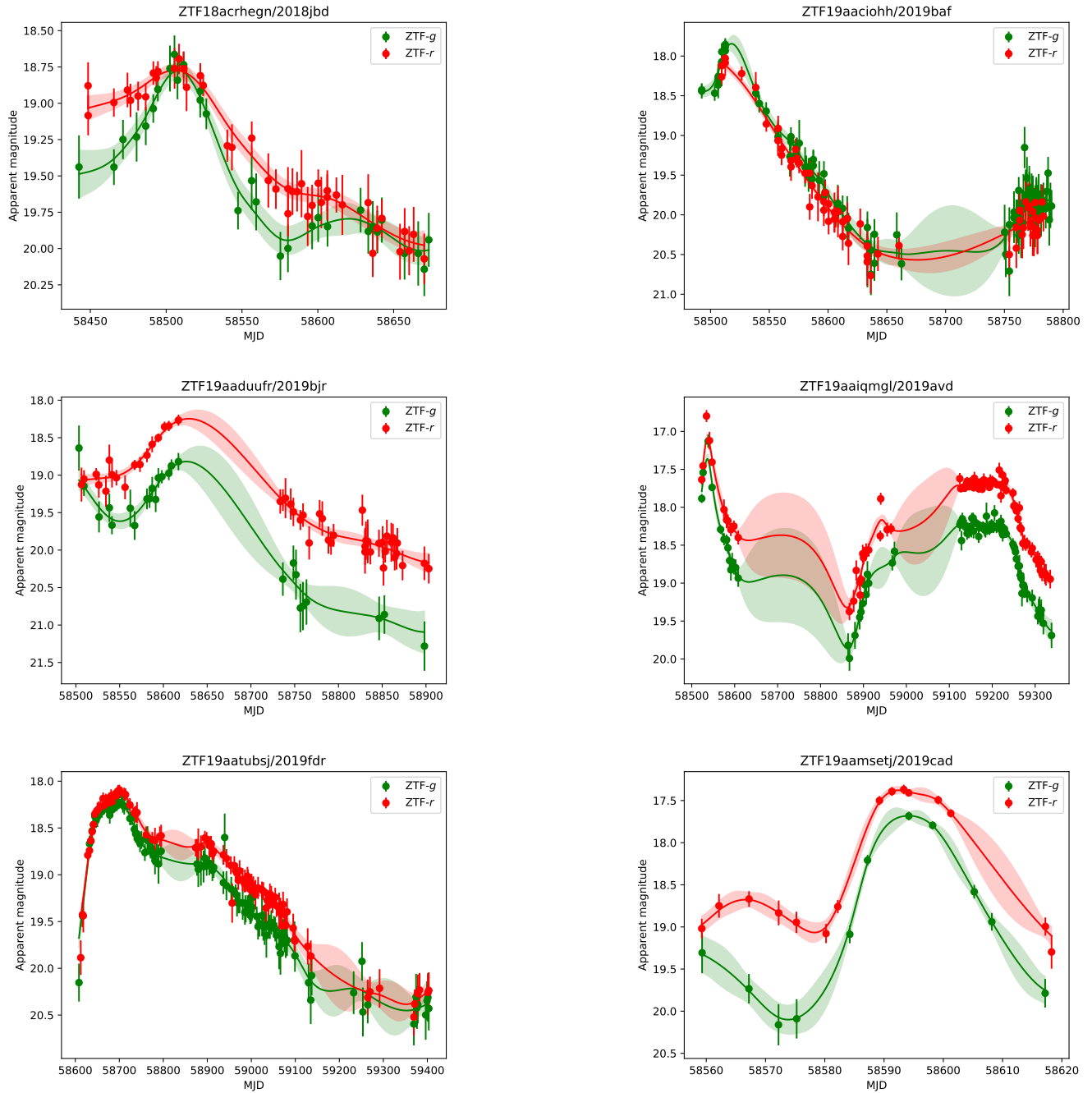


Figure 5. ZTF light curves of bumpy extragalactic transients. The lines and symbols are similar to those in Fig. 1. Details of the individual sources are given in Table 1.

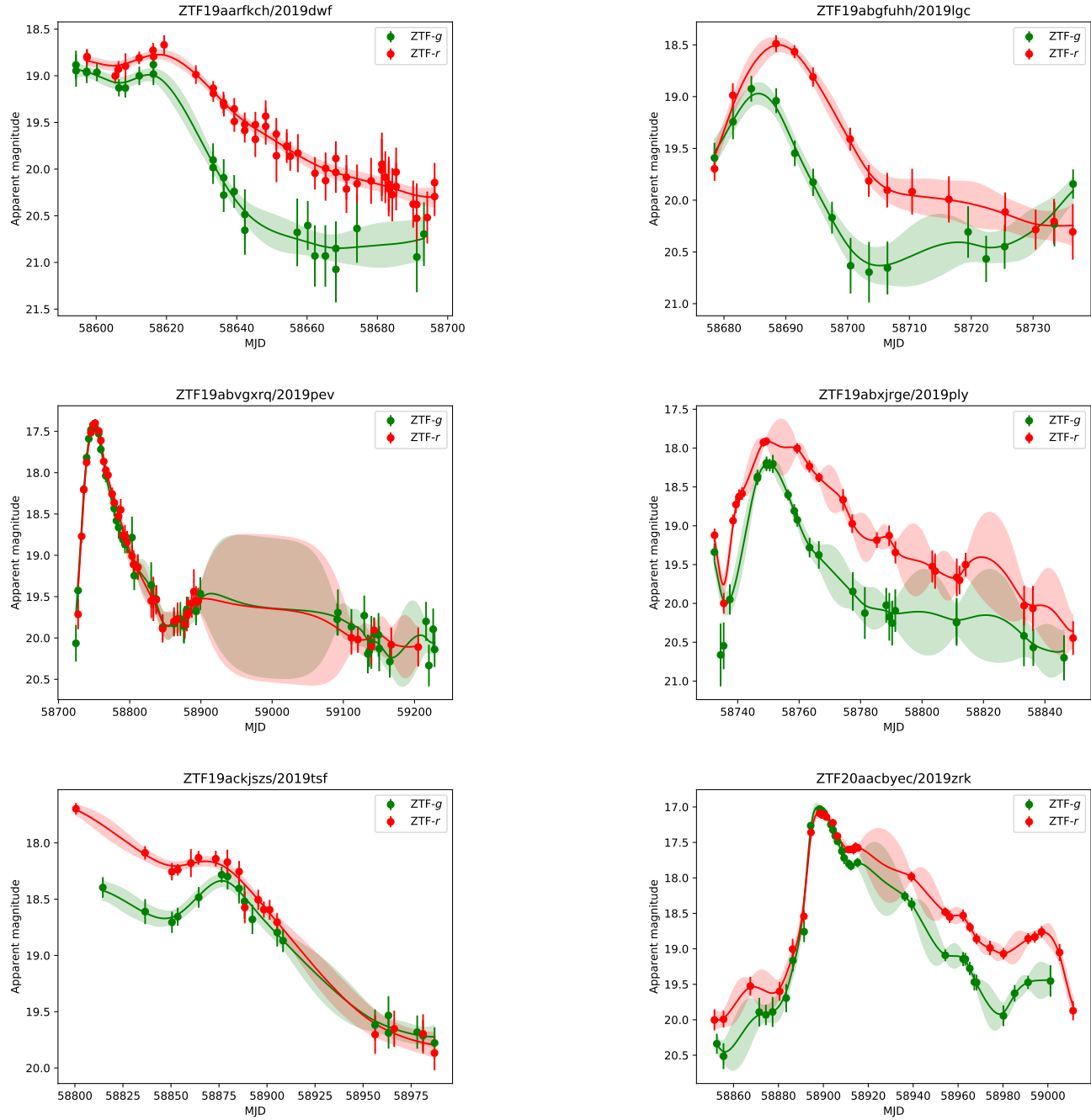


Figure 5. continued

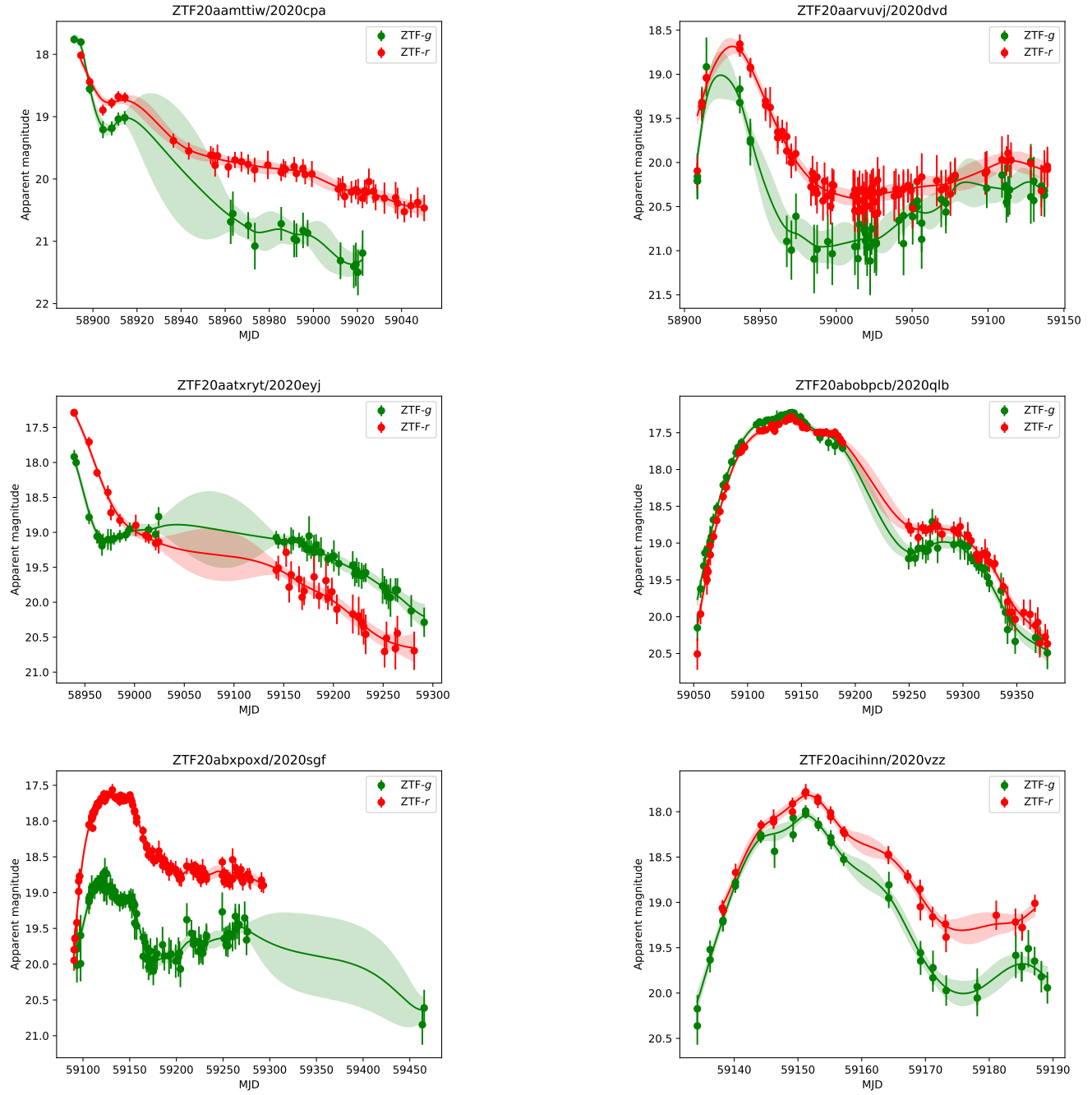


Figure 5. continued

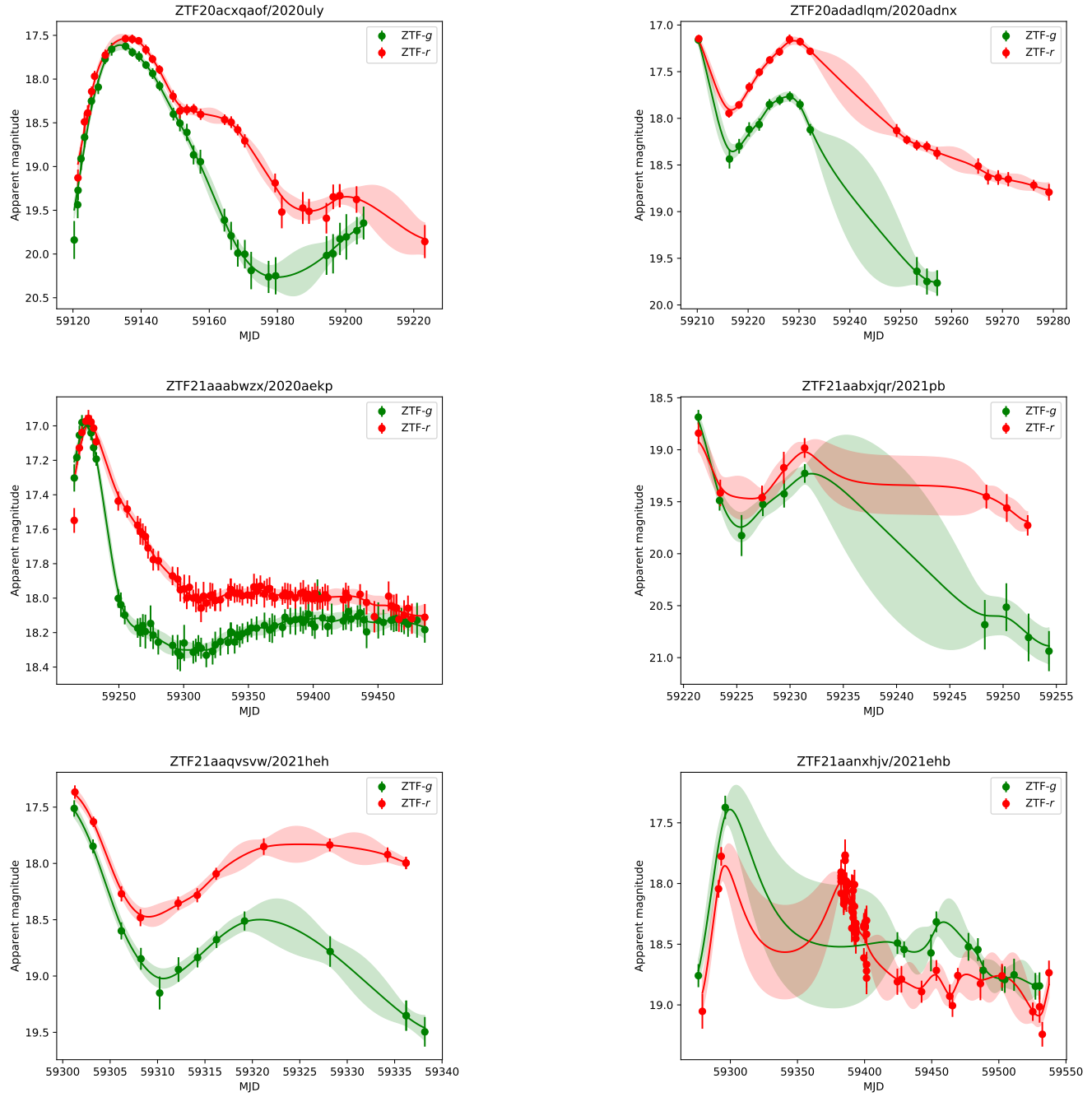


Figure 5. continued

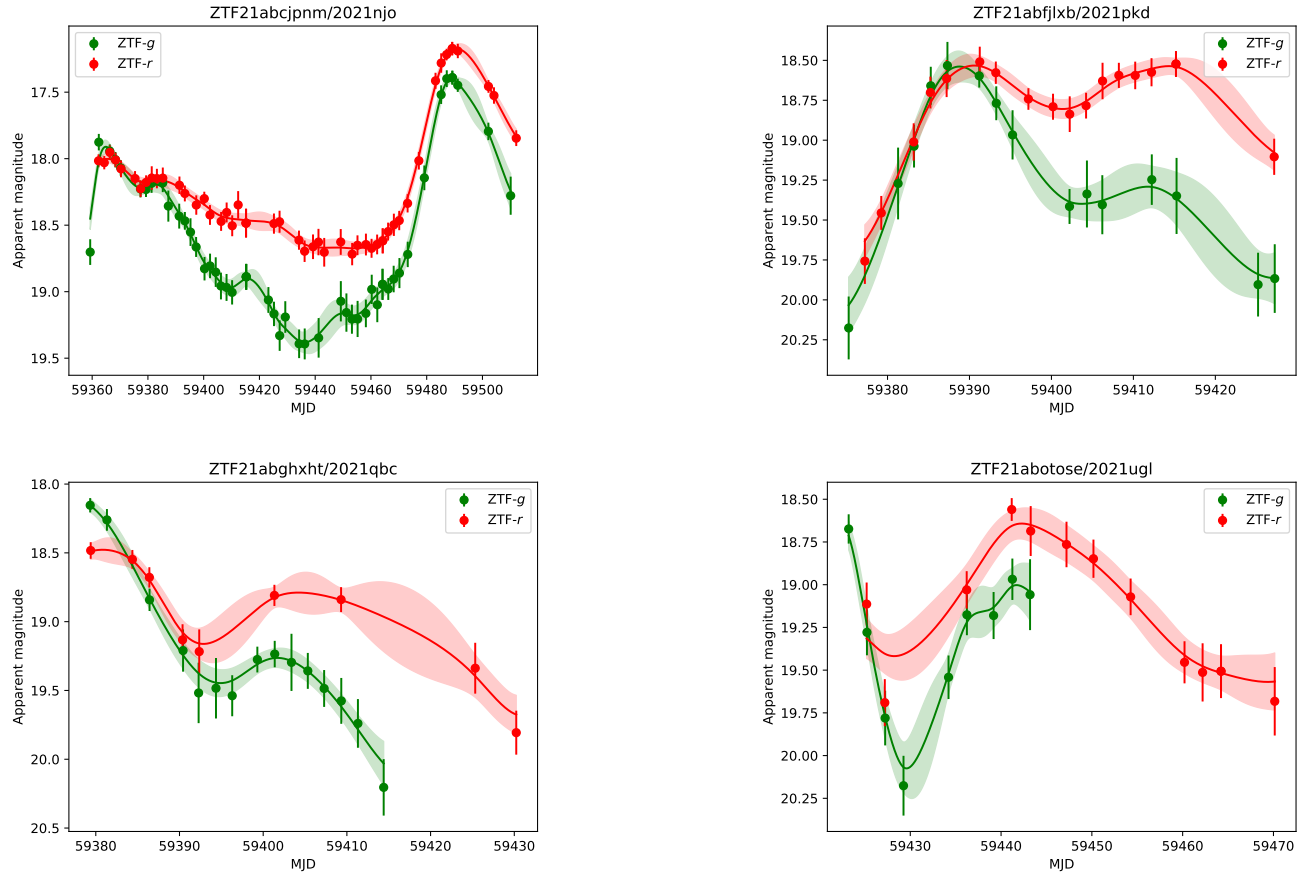


Figure 5. continued